Investigation of β-Substitution Activity of *O*-Acetylserine Sulfhydrolase from *Citrullus vulgaris*

Jamorious L. Smith,[a] Isa Madrigal Harrison,[a] Craig A. Bingman,[b] and Andrew R. Buller*[a]

Pyridoxal-5′-phosphate (PLP)-dependent enzymes have garnered interest for their ability to synthesize non-standard amino acids (nsAAs). One such class of enzymes, *O*-acetylserine sulfhydrylases (OASSs), catalyzes the final step in the biosynthesis of L-cysteine. Here, we examine the β-substitution capability of the OASS from *Citrullus vulgaris* (*Cv*OASS), a putative L-mimosine synthase. While the previously reported mimosine synthase activity was not reproducible in our hands, we successfully identified non-native reactivity with a variety of *O*-nucleophiles. Optimization of reaction conditions for carboxylate and phenolate substrates led to distinct conditions that were leveraged for the preparative-scale synthesis of nsAAs. We further show this enzyme is capable of C–C bond formation through a β-alkylation reaction with an activated nitroalkane. To facilitate understanding of this enzyme, we determined the crystal structure of the enzyme bound to PLP as the internal aldimine at 1.55 Å, revealing key features of the active site and providing information that may guide subsequent development of *Cv*OASS as a practical biocatalyst.

Introduction

Amino acids are the building blocks of proteins, natural products, and diverse industrially- and pharmaceutically relevant compounds.[1–3] The 20 standard amino acids are often modified synthetically and in Nature to yield non-standard amino acids, nsAAs.[4] nsAAs are used as molecular biological tools such as reporter molecules and fluorescence probes.[5–7] These molecules are prevalent in pharmaceuticals which has made developing synthetic routes to these compounds of great interest (Figure 1). While there are excellent synthetic methods to access many nsAAs,[8–10] biocatalytic routes offer distinct advantages. Enzymes operate under mild conditions with no protecting groups and can be combined in cascades to build complex molecules from simple precursors in a regio- and stereoselective fashion.[11–13] Identifying and characterizing new classes of enzymes that can meet the demands of preparative-scale synthesis will provide additional tools for the facile synthesis of desirable nsAAs.

Pyridoxal 5′-phosphate (PLP)-dependent enzymes found in Nature offer a unique alternative strategy to acquiring amino acids. This class of enzymes has been successfully used as biocatalysts to furnish nsAAs on preparative scale under relatively mild conditions.[12,14–17] Many members of the fold type II PLP-dependent enzymes catalyze β-replacement reaction to yield nsAAs.[15,18,19] A preeminent member of this family is the β-subunit of tryptophan synthase (TrpB), which has served as a model system for understanding PLP-dependent catalysis.[20–22] TrpB natively catalyzes β-substitution of the hydroxyl side chain of serine for indole through an electrophilic amino acrylate intermediate, E(A–A). Inspired by this highly selective C–C bond forming reaction, researchers have subjected TrpB to extensive engineering for β-substitution with a variety of *C*-nucleophiles including indoles, nitroalkanes, and enols.[14,15,18,23] These TrpB enzymes often react less efficiently with *S*- and *N*-nucleophiles, and none are known to catalyze β-replacement with *O*-nucleophiles.[19,24,25] Given that the products of such reactions are desirable building blocks, we considered the synthetic potential of other enzymes from the fold type II family.

O-Acetylserine sulfhydrolases (OASSs) are fold type II PLP enzymes that perform the final step in the biosynthesis of L-cysteine (Cys). As their name suggests, these enzymes bind *O*-acetylserine (OAS) and catalyze elimination of acetate to produce an electrophilic amino acrylate intermediate, E(A–A). Spectroscopic studies of OASS from *Salmonella typhimurium* (*St*OASS) have shown that *St*OASS forms a different tautomer of E(A–A) relative to TrpB, suggesting the potential for distinct chemistry.[26] OASS enzymes have previously been shown to operate with a variety of *S*- and *N*-nucleophiles.[27,28] Single-turnover kinetic analysis have further shown *St*OASS can promote β-substitution with *O*-nucleophiles. Traditional syntheses of β-*O*-substituted nsAAs generally feature protection steps and can generate undesirable byproducts.[29] While the prior mechanistic analyses of OASS suggest the potential for a useful catalyst, additional challenges must be overcome to develop an enzyme for preparative scale synthesis.[30,31] In particular, low conversion, product inhibition, and deleterious side reactivity

[a] J. L. Smith, I. M. Harrison, A. R. Buller
Department of Chemistry
University of Wisconsin-Madison
1101 University Avenue, Madison, Wisconsin 53706 (USA)
E-mail: arbuller@wisc.edu
[b] C. A. Bingman
Department of Biochemistry
University of Wisconsin-Madison
433 Babcock Drive, Madison, Wisconsin 53706 (USA)

Supporting information for this article is available on the WWW under https://doi.org/10.1002/cbic.202200157.

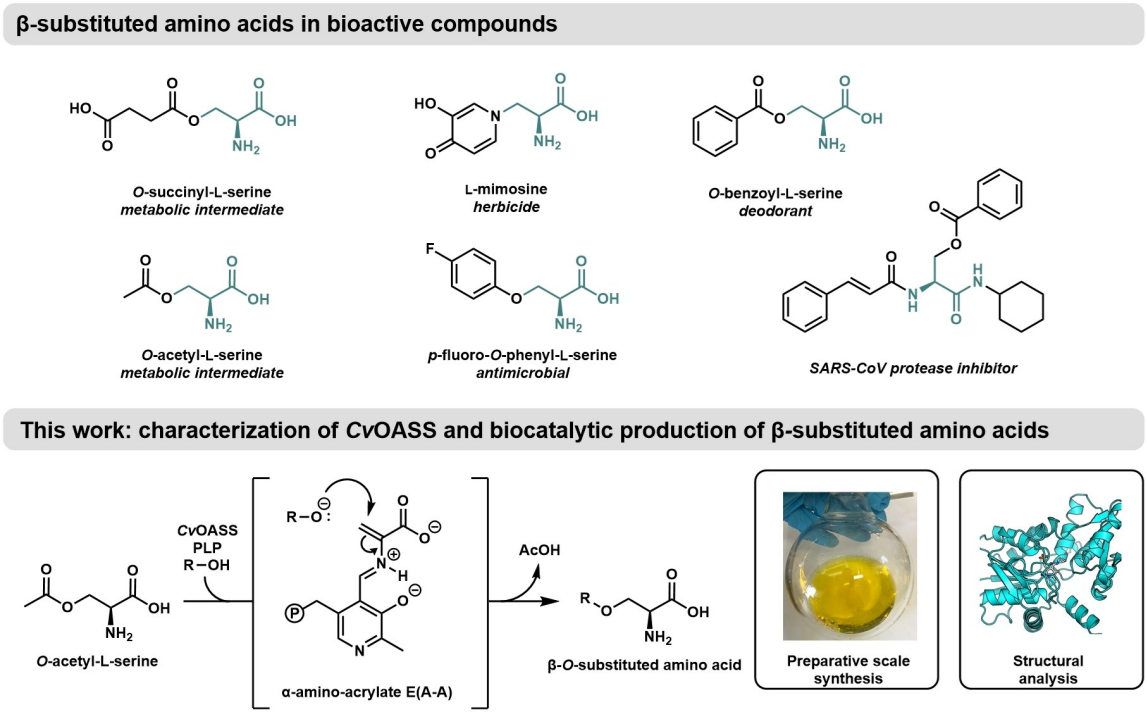

Figure 1. β-Substituted amino acids found in Nature and bioactive compounds; and synthesis of β-substituted amino acids using *Citrullus vulgaris O*-acetyl serine sulfhydrolase.

are all factors that potentially restrict the use of OASSs for preparative scale synthesis of nsAAs.

Here, we explored the biocatalytic properties of OASS from *Citrullus vulgaris* (*Cv*OASS, Figure 1). Previously, this enzyme was reported to catalyze the β-*N*-substitution of OAS to form L-mimosine, an herbicidal nsAA.[32,33] We obtained *Cv*OASS to explore mimosine synthase activity. We next tested the capability of *Cv*OASS to catalyze β-substitution with *O*-nucleophiles, a previously unexplored reaction for preparative scale synthesis. We then identifed reaction conditions that improve yields and enable productive β-substitution activity with *O*-nucleophiles including phenolates and carboxylates. We also observed an adventitious C–C bond forming reaction using (nitromethyl)benzene. We determined the X-ray crystal structure of *Cv*OASS at 1.55-Å resolution and, combined with mechanistic analyses, our studies provide a foundation for future development of this enzyme as a complementary biocatalyst for the synthesis of new β-substituted nsAAs.

Results and Discussion

O-acetylserine sulfhydrolase from *Citrullus vulgaris* catalyzes β-*O*-substitution

We heterologously expressed C-6-His tagged *Cv*OASS in *E. coli* BL21 (DE3). Purification by Ni-affinity chromatography reproducibly yielded ~80 mg purified protein per L culture (Figure S1). Previously, it was reported this enzyme catalyzed β-N-substitution of OAS with 3,4-dihydroxypyridine to yield L-mimosine.[28,33] However, analysis of this reaction in the presence of purified *Cv*OASS via UPLC-MS failed to identify L-mimosine (Figure S2). Upon screening with an alternative N-nucleophile, pyrazole, we observed clear evidence of *Cv*OASS-dependent product formation to produce the β-N-substituted nsAA, (β-pyrazol-1-yl)-L-alanine under previously reported conditions (Figure S6).

Undeterred by the lack of mimosine synthase activity, we considered alternative biocatalytic uses of the enzyme. In pioneering work, Maier showed that OASS homologues from diverse species are capable of efficient N- and S- substitution reactions and can be utilized for g-scale product formation through fermentation.[27] Previously, pre-steady state rapid kinetic analysis indicated that OASS from *Salmonella typhimurium* could perform a single turnover with a variety of C-, N-, O-, and S- nucleophiles.[30] Initial screening with a panel of substrates suggested that *Cv*OASS would be a good candidate for identification of new activities with OASSs (Figures S11–24). Co-injections with authentic β-*O*-phenyl-L-serine and tyrosine confirmed the *Cv*OASS-dependent O-substitution reaction with phenol (Figure S3). Intrigued by the potential of this well-expressing enzyme to react with O-nucleophiles, we sought to optimize reaction conditions for preparative-scale synthesis.

Preparative scale β-substitution with phenols

Initial reactions with phenol were performed in 100 mM KP_i buffer pH 7.0 at 10 mM phenol, 20 mM OAS, and 10 μM *Cv*OASS

(0.1 mol%, 1000 max TON). The product was purified using reverse phase chromatography in approximately 20% isolated yield. This low yield prompted us to consider factors that may hinder *Cv*OASS reactivity. A 0.25 mol% catalyst loading resulted in an improved UPLC-MS-PDA yield of 51% after 2.5 hours. Variation of the catalyst loading showed enzymatic turnover was limiting yield under these conditions (Figure 2A, entries 1–3).

We next considered the complex effects of pH on the reaction progress. As the pK_a of phenol is 10 and reactions were performed at pH 7.0, increasing the pH of the reaction would increase the concentration of the nucleophilic phenolate and potentially enhance the reaction rates and yield. In addition, we observed a decrease in substrate conversion via UPLC–MS after approximately 2.5 hours at pH 8.0, which may suggest product re-entry into the catalytic cycle and degradation. Indeed, at pH 8.0, we observed an increase in yield by up to 71% after 2 hours (Figure 2A, entries 2–4). To circumvent these issues, we performed time course experiments at a range of pH values to observe product formation and degradation (Figure 2B). Increasing the pH to 8.0 and quenching the reaction after 2.5 hours resulted in a 2-fold boost in activity without significant product degradation.

Next, we tested the effects of various co-solvents. Although phenol is soluble in water, other analogs may benefit from the addition of organic solvent. We observed complete loss of activity upon the addition of ethanol. Similarly, addition of 5% dimethyl sulfoxide (DMSO) or acetonitrile reduced the yields of the reaction. An additional limitation to this reaction was the intrinsic instability of the starting material, which can undergo an O→N acyl shift (Figure 3B). We observed no substantial increase in product formation when increasing the stoichiometric ratio of OAS relative to the nucleophile. Nevertheless, we decided to maintain excess amounts of OAS in our final conditions to diminish product re-entry into the catalytic cycle. Together, these conditions enabled the formation of the β-*O*-substituted amino acid product with a 60% isolated yield by reverse-phase chromatography. We next sought to identify conditions that were conducive to β-*O*-substitution with another class of oxygen nucleophiles used in the pre-steady state rapid kinetic analysis of OASSs, carboxylates.[30]

A

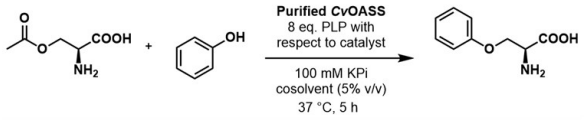

entry	Catalyst loading (mol % cat.)	pH	cosolvent	HPLC Yield
1	0.1	7.0	no cosolvent	18%
2	0.25	6.5	no cosolvent	36%
3	0.25	7.0	no cosolvent	51%
4	0.25	8.0	no cosolvent	71%
5	0.25	8.0	EtOH	0%
6	0.25	8.0	DMSO	55%
7	0.25	8.0	MeCN	58%

B

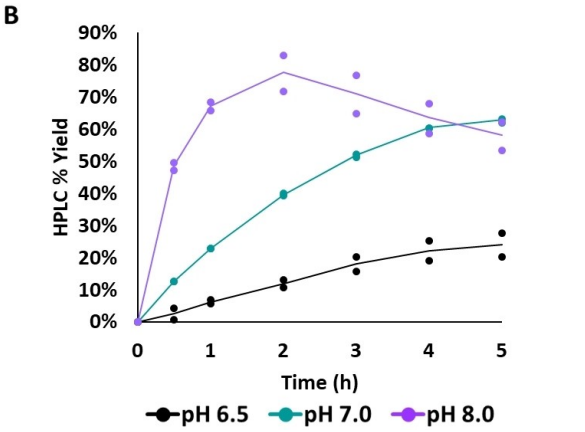

Figure 2. Analytical scale optimization of *Cv*OASS-catalyzed β-*O*-substitution with phenol. A. Table representing various conditions sampled for the phenol β-O-substitution reaction. Reactions were run with 10 mM phenol, 20 mM OAS, 100 mM KP_i pH 7–8.0 and 0.1-0.25 mol% cat. Loading for 5 hours. Conversion values are reported as the average of duplicate experiments after 2 hours. B. Progress curve for the synthesis of *O*-phenyl-Ser as a function of pH. Reactions conditions correspond to entries 2–4 in the neighboring table. HPLC yields were calculated based on *O*-phenyl-L-serine standard curve (Figure S4).

A

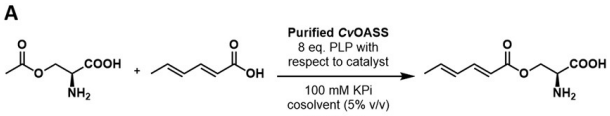

entry	Catalyst loading (mol % cat.)	pH	cosolvent	Apparent Yield
1	0.25	8.0	MeCN	17%
2	0.1	7.0	no cosolvent	11%
3	0.25	7.0	no cosolvent	17%
4	1.0	7.0	no cosolvent	15%
5	1.0	7.5	no cosolvent	17%
6	1.0	8.0	no cosolvent	0%
7	1.0	6.5	no cosolvent	32%
8	1.0	6.5	EtOH	0%
9	1.0	6.5	DMSO	19 %
10	1.0	6.5	MeCN	0%

B

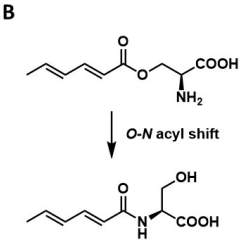

C

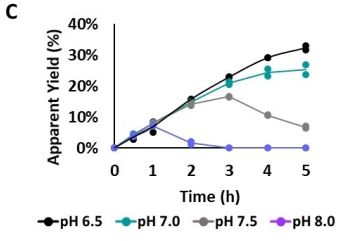

Figure 3. Analytical scale optimization of *Cv*OASS-catalyzed β-*O*-substitution with sorbic acid. A. Analytical scale optimization of *Cv*OASS-catalyzed β-*O*-substitution reactions with sorbic acid Conditions: 10 mM sorbic acid, 20 mM OAS, 100 mM KPi pH 7–8.0 or 100 mM PIPES pH 6.5 and 0.1–1.0 mol% cat. loading, with 5% (v/v) co-solvent for five hours. B. O→N acyl shift of β-O-substituted amino acid. C. 5-hour time course data corresponding to phenol reaction optimization table (see Figure 3A) Apparent yields were calculated by dividing total absorbance of product at 280 nm divided by total product and sorbic acid absorbance at 280 nm. Table values are reported as the average of duplicate experiments after 5 hours.

Lower pH and higher catalyst loading enable isolation of ester products

We initially screened for activity with a panel of carboxylate-containing compounds. Although we were able to observe distinct MS signals corresponding to the predicted β-*O*-substituted products, we were initially unable to purify compounds from the panel due to low (<5%) conversion. *Cv*OASS had promising activity on sorbic acid using the same initial conditions as for phenol, resulting in up to 11% apparent yield (Figure 3A, entry 1). However, there was pronounced product degradation via the O→N acyl shift during purification, prompting us to identify conditions that would mitigate the inherent instability of the ester products and consequently raise yield (Figure 3B). Although authentic product was unavailable for generation of a standard curve prior to reaction condition optimization, we were able to track reaction progress using the prominent absorbance of sorbic acid at 280 nm. For determination of optimal β-*O*-substitution reaction conditions with carboxylic acids, which are more acidic than phenols, we first rescreened the catalyst loading and determined that 1.0 mol% catalyst increased yield. We monitored for improved activity on a range of pH values over a 5-hour time course (Figure 3C). Conditions exceeding pH 7.0 resulted in degradation of the product over time. We observed a modest improvement in apparent yield up to 32% by lowering the pH to 6.5. These conditions were chosen to prevent considerable loss of the starting material while obtaining the highest conversion possible. The addition of co-solvents, DMSO and ethanol, again resulted in diminished activity. Although use of acetonitrile as a co-solvent greatly improved starting material solubility, it effectively abolished β-*O*-substitution activity with carboxylate-containing compounds. On preparative scale, we isolated the product of β-*O*-substitution with sorbate in 29% yield. Trace activity was also observed with a panel of carboxylic acids. Unfortunately, conversion remained low with other carboxylic acid substrates we tested using our optimized conditions, prompting us not to further pursue purification of these compounds (Figure S6).

*Cv*OASS can catalyze β-substitution with a variety of nucleophiles

Having explored the capacity of *Cv*OASS to catalyze β-*O*-substitution, we screened for reactivity with several potential nucleophiles. We observed clear C–C bond formation via a β-alkylation reaction using (nitromethyl)benzene through a formal nucleophilic substitution reaction (Figure 4). We observed good reactivity with this substrate under the basic conditions originally developed for phenols, and successfully isolated γ-NO_2-homophenylalanine at 45% yield. We opted not to perform reaction optimization for this substrate. We also used these conditions for isolation on preparative scale with phenol and *m*-cresol. Reactions with these substrates gave the corresponding β-*O*-substituted nsAAs in 60% and 22%, respectively (Figure 4). We attributed the decrease in activity to steric clashes between the bulkier functional groups on substituted phenols and the enzyme active site residues. Trace activity was observed with a panel of related phenols (Figure S6). However, their apparent conversion was <5%, prompting us not to pursue isolation. We also screened for C–N bond formation with aniline analogues, but no activity was observed. To affirm that the enzyme could perform C–S bond formation, we additionally screened for activity using the thiophenol. We observed clear evidence of product formation via UPLC-MS for this nucleophile but did not pursue preparative scale synthesis as this type of reaction has been extensively studied.[27]

Last, we explored the enantioselectivity of the *Cv*OASS transformation. Enantioselectivity was determined through derivatization using Marfey's reagent (1-fluoro-2-4-dinitrophenyl-5-L-alanine amide, L-FDAA), followed by UPLC-MS analysis.[34,35] In the case of the (nitromethyl)benzene product, derivatization also allowed for separation and quantitation of the diastereomers from this reaction (Figures S7–S10). Based on this analysis, we confirmed >99% enantiomeric excess (ee) for the C–O and C–C bond forming reactions and a diastereomeric ratio (dr) of 68:32 for the (nitromethyl)benzene product. This ratio is likely an underestimate of the enzymatic diastereoselectivity because the product can epimerize in aqueous solutions.[15]

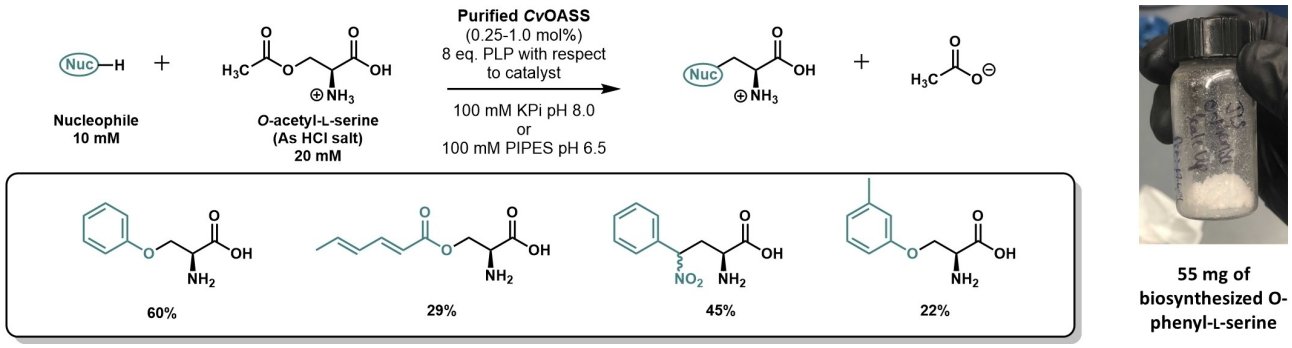

55 mg of biosynthesized O-phenyl-L-serine

Figure 4. Preparative scale synthesis of nsAAs with *Cv*OASS. Reactions with phenols and (nitromethyl)benzene were performed at pH 8.0 with 0.25 mol% catalyst. The reaction with sorbic acid was performed at pH 6.5 with 1.0 mol% catalyst. Isolated yields are given.

Spectroscopic studies of catalytic intermediates

To gain insights into the reactivity of *Cv*OASS, we used UV/vis spectroscopy to probe the catalytic mechanism. *Cv*OASS is a PLP-dependent enzyme, and the catalytic intermediates possess distinct spectroscopic signals (Figure 5A). In the absence of substrate, *Cv*OASS is bound to PLP as the internal aldimine E(Ain) with a λ_{max} at 412 nm (Figure 5B).[30] Upon the addition of OAS, we observed an immediate decrease of the peak at 412 nm and rapid appearance of two new peaks with λ_{max} values at 325 nm and 460 nm. We attribute these new peaks to the formation of an α-aminoacrylate E(A–A) intermediate.

These data are also consistent with previous work on related OASS.[30,31,36] We then added a nucleophilic substrate, succinate, which resulted in another spectral shift and a new peak with a λ_{max} value of 380 nm. We assign this peak to the formation of a product-bound external aldimine.

*Cv*OASS active site reveals binding interactions that support formation of functionalized serine analogues

We next used X-ray crystallography to understand the structural features of *Cv*OASS that give rise to reactivity. Sparse matrix screening of crystallographic conditions revealed that 0.1 M phosphate/citrate at pH 4.2 with 40% PEG 300 produced high quality crystals of *C*-His-*Cv*OASS. Crystals were reproduced via sitting drop vapor diffusion; subsequent harvesting and diffraction yielded data up to 1.55-Å resolution. The structure was solved by molecular replacement with a homolog (PDB ID: 1Z7Y, 83.4% identity). The enzyme was crystallized as a homodimer with one protomer in the asymmetric unit. The enzyme fold is consistent with the fold of other members of the fold-type II family of PLP-dependent proteins. The crystal structure revealed several features of the enzyme.

The PLP cofactor was linked to Lys49 in an internal Schiff base. We observed that the active site of *Cv*OASS was exposed to solvent and citrate was non-covalently bound in the active site with a carboxylate mimicking the predicted binding pose of an amino acid substrate (Figure 5C). Additionally, we observed a crown-ether type complex on the surface of the protein between Lys194 and a single polyethylene glycol 300 molecule (Figure S5). We attempted substrate soaking with OAS. However, crystals were unstable to this perturbation. Instead, to gain insight into the potential substrate binding motifs, we built a computational model with the *O*-phenyl-L-serine external aldimine bound in the active site. The external aldimine was well accommodated by the active site indicating potential

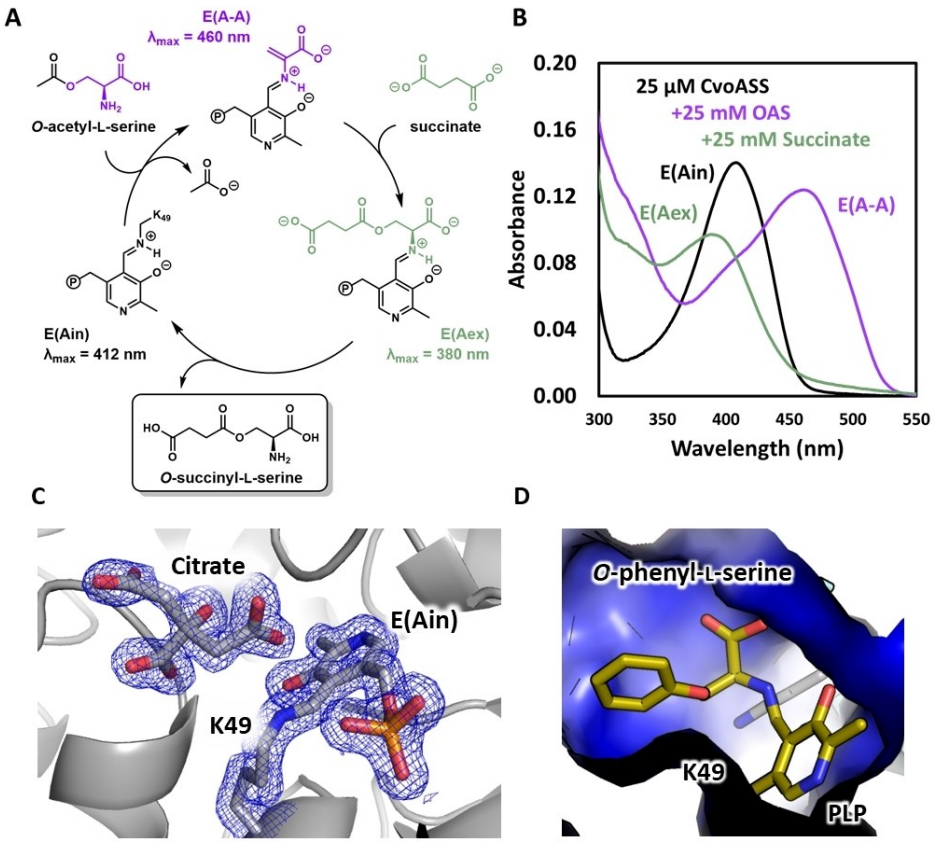

Figure 5. Structural characterization of *Cv*OASS. A. Mechanism of β-*O*-substitution with *Cv*OASS. B. UV/Vis spectra of *Cv*OASS upon the addition of pro-electrophile, OAS, and succinate. C. Crystal structure of *Cv*OASS at 1.55-Å resolution in the PLP-internal aldimine state with citrate bound into the active site of the enzyme contoured at 1.5σ PDB ID: 7N2T. D. Model of *Cv*OASS in the PLP-external aldimine state with *O*-phenyl-L-serine at the cleft of the active site. Electrostatic surface potential of *Cv*OASS's active site channel depicted in blue and black.

interactions that could be targeted for subsequent engineering studies to alter the scope or selectivity of the enzyme (Figure 5D).

Conclusion

Here, we demonstrated the utility of *Cv*OASS for the preparative scale synthesis of β-*O*-substituted amino acids. By studying enzymes from a different class of the fold-type II family, we observed that *Cv*OASS can be added to the repertoire of fold-type II PLP-dependent biocatalysts capable of non-native activity to produce diverse nsAAs. We show evidence that *Cv*OASS exhibits activity with several *O*-, *N*-, and *S*-nucleophiles. We also identify modest activity with a nitroalkane compound demonstrating the potential of *Cv*OASS as a C–C bond forming catalyst. Spectrophotometric measurements revealed key PLP-dependent intermediates and are consistent with previously reported literature.[30] These data also reveal a different tautomer for the reactive α-amino-acrylate intermediate of *Cv*OASS compared to TrpB, which may be related to their distinct chemoselectivity.

Reaction condition optimizations led to processes capable of amino acid production at mg scale. Additionally, the identification of unique reaction conditions based on the pK_a of the conjugate acid of the nucleophile provide a clear basis for extending the reactivity reported here to new substrates. We also report the crystal structure for *Cv*OASS, which can be used to inform future engineering efforts. These data may serve as a starting point for future protein engineering studies, that may further expand the scope of β-substituted amino acids that can be produced through sustainable biocatalysis.

Experimental Section

All chemicals and reagents were purchased from commercial suppliers (Sigma-Aldrich, VWR) at the highest quality available and used without further purification unless stated otherwise. Genes were purchased as gBlocks from Integrated DNA Technologies (IDT). *E. coli* cells were electroporated with an Eppendorf E-porator at 2500 V. New Brunswick I26R shaker incubators (Eppendorf) were used for cell growth. Cell disruption via sonication was performed with a Sonic Dismembrator 550 (Fisher Scientific) sonicator. UV-vis spectroscopic measurements were collected on a UV-2600 Shimadzu spectrophotometer. Optical density measurements were collected using an Ultraspec 10 Cell density meter (Amersham Biosciences). Ultrahigh pressure liquid chromatography-mass spectrometry (UPLC-MS) data were collected on an Acquity UPLC (Waters) equipped with an Acquity PDA and QDA MS detector using either an Intrada Amino Acid column (Imtakt) or a BEH C18 column (Waters). Preparative-scale flash chromatography was performed on an Isolera One Flash Purification system (Biotage). NMR data were collected on Bruker e400 or 500 MHz spectrometers equipped with BBFO and DCH cryoprobes, respectively. All NMR chemical shifts were referenced either to a residual solvent peak or TMS internal standard. Spectra recorded using DMSO-d^6 were referenced to the residual DMSO signal at 2.5 ppm for ^{1}H and 39.52 ppm for ^{13}C NMR spectroscopy. Signal positions were recorded in ppm with the abbreviations s, d, t, q, dd, br, m, and app denoting singlet, doublet, triplet, quartet, doublet of doublets, broad, multiplet, and apparent respectively. All coupling constants *J* are measured in Hz. High resolution mass spectrometry data were collected with a Q Extractive Plus Orbitrap (NIH 1S10OD020022-1) instrument with samples ionized by ESI.

Acknowledgements

We thank Dr. Tyler Doyon, Allwin McDonald, Jon Ellis, and the rest of the Buller laboratory for stimulating discussions about PLP chemistry, day-to-day guidance, and editing of the manuscript. We acknowledge support of an L&S Community of Graduate Research Scholars Fellowship and the National Institutes of Health (NIH) Chemistry-Biology Interface Training Program (CBI) Traineeship (to J.L.S.). This research was additionally funded with the support of the Wisconsin Alumni Research Foundation and the National Institutes of Health (DP2-GM137417), to A.R.B.

Conflict of Interest

The authors declare no conflict of interest.

Data Availability Statement

The data that support the findings of this study are available from the corresponding author upon reasonable request.

Keywords: beta-substitution · biocatalysis · biosynthesis · enzymology · PLP

[1] A. J. Rose, *Nutrition* **2019**, *11*, 2623.
[2] H. Konno, M. Wakabayashi, D. Takanuma, Y. Saito, K. Akaji, *Bioorg. Med. Chem.* **2016**, *24*, 1241–1254.
[3] K. Akaji, H. Konno, *Molecules* **2020**, *25*, 3920.
[4] A. Dumas, L. Lercher, C. D. Spicer, B. G. Davis, *Chem. Sci.* **2015**, *6*, 50–69.
[5] C. Albayrak, J. R. Swartz, *Nucleic Acids Res.* **2013**, *41*, 5949–5963.
[6] F. Agostini, J. S. Völler, B. Koksch, C. G. Acevedo-Rocha, V. Kubyshkin, N. Budisa, *Angew. Chem. Int. Ed.* **2017**, *56*, 9680–9703; *Angew. Chem.* **2017**, *129*, 9810–9835.
[7] X. Jin, O. J. Park, S. H. Hong, *Appl. Microbiol. Biotechnol.* **2019**, *103*, 2947–2958.
[8] Y. Pérez-Fuertes, J. E. Taylor, D. A. Tickell, M. F. Mahon, S. D. Bull, T. D. James, *J. Org. Chem.* **2011**, *76*, 6038–6047.
[9] J. Chen, S. P. Corbin, N. J. Holman, *Org. Process Res. Dev.* **2005**, *9*, 185–187.
[10] K. J. M. Beresford, N. J. Church, D. W. Young, *Org. Biomol. Chem.* **2006**, *4*, 2888–2897.
[11] A. D. McDonald, L. J. Perkins, A. R. Buller, *ChemBioChem* **2019**, *20*, 1939–1944.
[12] P. Kumar, A. Meza, J. M. Ellis, G. A. Carlson, C. A. Bingman, A. R. Buller, *ACS Chem. Biol.* **2021**, *16*, 95.
[13] T. J. Doyon, P. Kumar, S. Thein, M. Kim, A. Stitgen, A. M. Grieger, C. Madigan, P. H. Willoughby, A. R. Buller, *ChemBioChem* **2022**, *23*, e202100577.
[14] A. R. Buller, S. Brinkmann-Chen, D. K. Romney, M. Herger, J. Murciano-Calles, F. H. Arnold, *Proc. Natl. Acad. Sci. USA* **2015**, *112*, 14599–14604.
[15] D. K. Romney, N. S. Sarai, F. H. Arnold, *ACS Catal.* **2019**, *9*, 8726–8730.
[16] D. K. Romney, J. Murciano-Calles, J. E. Wehrmüller, F. H. Arnold, *J. Am. Chem. Soc.* **2017**, *139*, 10769–10776.
[17] J. M. Ellis, M. E. Campbell, P. Kumar, E. P. Geunes, C. A. Bingman, A. R. Buller, *Nat. Catal.* **2022**, *5*, 136–143.

[18] D. K. Romney, J. Murciano-Calles, J. E. Wehrmüller, F. H. Arnold, *J. Am. Chem. Soc.* **2017**, *139*, 10769–10776.
[19] M. Herger, P. Van Roye, D. K. Romney, S. Brinkmann-Chen, A. R. Buller, F. H. Arnold, *J. Am. Chem. Soc.* **2016**, *138*, 8388–8391.
[20] B. G. Caulkins, R. P. Young, R. A. Kudla, C. Yang, T. J. Bittbauer, B. Bastin, E. Hilario, L. Fan, M. J. Marsella, M. F. Dunn, L. J. Mueller, *J. Am. Chem. Soc.* **2016**, *138*, 15214–15226.
[21] B. G. Caulkins, B. Bastin, C. Yang, T. J. Neubauer, R. P. Young, E. Hilario, Y. M. M. Huang, C. E. A. Chang, L. Fan, M. F. Dunn, et al., *J. Am. Chem. Soc.* **2014**, *136*, 12824–12827.
[22] J. B. Holmes, V. Liu, B. G. Caulkins, E. Hilario, R. K. Ghosh, V. N. Drago, R. P. Young, J. A. Romero, A. D. Gill, P. M. Bogie, et al., *Proc. Natl. Acad. Sci. USA* **2022**, *119*, e2109235119.
[23] E. J. Watkins-Dulaney, N. P. Dunham, S. Straathof, S. Turi, F. H. Arnold, A. R. Buller, *Angew. Chem.* **2021**, *133*, 21582–21587.
[24] C. E. Boville, R. A. Scheele, P. Koch, S. Brinkmann-Chen, A. R. Buller, F. H. Arnold, *Angew. Chem. Int. Ed.* **2018**, *57*, 14764–14768; *Angew. Chem.* **2018**, *130*, 14980–14984.
[25] P. J. Almhjell, C. E. Boville, F. H. Arnold, *Chem. Soc. Rev.* **2018**, *47*, 8980–8997.
[26] A. Klein, P. Rovó, V. V. Sakhrani, Y. Wang, J. B. Holmes, V. Liu, P. Skowronek, L. Kukuk, S. K. Vasa, P. Güntert, L. J. Mueller, R. Linser, *Proc. Natl. Acad. Sci. USA* **2022**, *119*, e2114690119.
[27] T. H. P. Maier, *Nat. Biotechnol.* **2003**, *21*, 422–427.
[28] M. Noji, I. Murakoshi, K. Saito, *Biochem. Biophys. Res. Commun.* **1993**, *197*, 1111–1117.
[29] T. E. Kristensen, *Beilstein J. Org. Chem.* **2015**, *11*, 446–468.
[30] W. M. Rabeh, S. S. Alguindigue, P. F. Cook, *Biochemistry* **2005**, *44*, 5541–5550.
[31] W. M. Rabeh, P. F. Cook, *J. Biol. Chem.* **2004**, *279*, 26803–26806.
[32] T. Dang, S. Tawata, T. Dang, in *Herbicides: Advances in Research*, InTech, **2013**.
[33] K. Saito, N. Kimura, F. Ikegami, M. Noji, *Biol. Pharm. Bull.* **1997**, *20*, 47–53.
[34] R. Bhushan, H. Brückner, *Amino Acids* **2004**, *27*, 231–247.
[35] P. Marfey, *Carlsberg Res. Commun.* **1984**, *49*, 591–596.
[36] A. Chattopadhyay, M. Meier, S. Ivaninskii, P. Burkhard, F. Speroni, B. Campanini, S. Bettati, A. Mozzarelli, W. M. Rabeh, L. Li, et al., *Biochemistry* **2007**, *46*, 8315–8330.

Manuscript received: March 20, 2022
Revised manuscript received: April 24, 2022
Accepted manuscript online: April 27, 2022
Version of record online: June 1, 2022